

A DFT Study on the Structural and Electronic properties of Cadmium Telluride (Cd_nTe_n) and Cadmium Zinc Telluride ($\text{Cd}_{(n-m)}\text{Zn}_m\text{Te}_n$) Clusters

Menbere Weldetsadik¹ and Hagos Woldegebriel^{2*}

¹Department of Physics, CNCS, Wolkitie University, Wolkitie, Ethiopia, menbieran@yahoo.com

²Department of Physics, CNCS, P.O. Box 231, Mekelle University, Mekelle, Ethiopia (*hagos93@mu.edu.et).

ABSTRACT

In this study, the structural and electronic properties of Cd_nTe_n and $\text{Cd}_{(n-m)}\text{Zn}_m\text{Te}_n$ clusters have been studied using the plane wave based density functional theory (DFT). The QUANTUM ESPRESSO/PWSCF package employing the local density approximation (LDA) for the exchange correlation potential is used. In all calculations, the geometry optimization was employed in allowing the structures to fully relax. Structural properties viz. geometry, bond length and electronic properties like HOMO-LUMO gap, binding energy, second order energy difference and nature of bonding have been analyzed. As a result, we obtained that the binding energy increases with increasing cluster size and doping level. Zinc doped Cd_nTe_n clusters show greater binding energy than the undoped clusters. Planar structures are obtained for very small cluster sizes and in our simulation three dimensional structure is found at Cd_4Te_4 cluster in the lowest energy geometry. Clusters of certain sizes often have special properties, i.e. higher stability or larger HOMO-LUMO gap when compared with other clusters, such as $\text{Cd}_{(3-m)}\text{Zn}_m\text{Te}_3$, $m = 0, 1, 2$ clusters. Thus, we can take it as a building block in the growth of the structures in our calculation. The partial charge density distribution of the HOMO and LUMO levels for Cd_nTe_n and $\text{Cd}_{(n-m)}\text{Zn}_m\text{Te}_n$ clusters show that, the HOMO levels are predominantly localized on the Te atoms and the LUMO levels are distributed on both Cd and Zn atoms. Moreover, the LUMO levels are delocalized at the center of the clusters due to the hybridization of the molecular orbitals. The LDOS and energy level plots show discrete lines at the atomic level and the discreteness disappears as the cluster size increases.

Keywords: HOMO-LUMO, Pseudopotential, Cluster, Isomer.

1. INTRODUCTION

Semiconductor nanoparticles or Quantum Dots (QDs), in particular II-VI materials, have received tremendous attention during the last decades owing to their unusual physical properties and wide range of applications. Hence, a systematic study of QDs is useful to understand the evolution of their physical and chemical properties with size. The relationship between the geometry and the electronic structure plays a critical role in dictating the properties of a material. Semiconductor clusters have been shown to exhibit exotic properties quite different from those in molecules and solids. Compared with homogeneous clusters such as carbon and silicon, heterogeneous semiconductor clusters like CadmiumTelluride are more attractive because their properties can be controlled by changing the composition. For these reasons, theoretical studies

on clusters are critical to the design and synthesis of advanced materials with desired optical, electronic and chemical properties.

The II-VI semiconductors are of great importance due to their applications in optoelectronics, solar cells, integrated optics and electro-optics devices. Hence, there are different experimental and theoretical studies on this group using various techniques or methods.

A number of theoretical and experimental attempts (Jianguang, 2009) have been made to determine the structure and properties of small Cd_nTe_n and related clusters. Most of the theoretical studies have been focused on clusters of a few atoms. According to Rusus (2006) on the study of structural, electronic transport and optical properties of Zn doped CdTe thin films, the non-doped CdTe thin films are found to be cubic oriented (111) polycrystalline structure whereas the doped ones are a quasi-amorphous structure as investigated using X-Ray Diffraction techniques.

The structural, electronic and optical properties of CdTe clusters were studied using thermal evaporation and deposition method and Shimadzu UV-365 spectrophotometer in photon energy ranging from 0.5-2.5eV. As a result, properties were dependent on the deposition parameter (Shreekanthan, 2006). Consequently, they mentioned low deposition rates were observed to result in hexagonal deposits whereas high rate of deposition favored cubic structure for the film. Similarly, Swati (2001) studied $Cd_{(1-x)}Zn_xTe$ crystals with $0 \leq x \leq 0.14$ alloys using photoluminescence (PL) spectroscopy (PL) and found that, increasing the doping concentration increased the energy gap (E_g) of the bulk crystal. According to Bhattacharya and Anjali (2007), small stoichiometric Cd_nTe_n clusters and a few nonstoichiometric Cd_mTe_n (for $m, n = 1, 4, 13, 16, 19$ and $m \neq n$) clusters have been studied using the density functional formalism and projector augmented wave method within the generalized gradient approximation. They observed that, upon relaxation, the symmetry changes for the Cd-rich clusters whereas the Te-rich clusters retain their symmetry.

Theoretical studies of heterogeneous semiconductor clusters have been limited due to computational difficulties arising from the large number of structural and permutational isomers formed due to multiple elements. On one hand, sophisticated computational methods such as self-consistent quantum mechanical calculation is required to make reliable prediction on the properties of these clusters in the absence of comprehensive experimental results. On the other

hand, the amount of computational work is enormous in order to find all the stable isomers for a given cluster size and composition. Semiconductor nanoparticle materials are important in designing of novel photoelectrochemical devices based upon surface-derivitized nanoparticle films (Douglas et al., 1997).

In this work, we present a systematic study on the electronic and structural properties of Cadmium Telluride and Cadmium Zinc Telluride clusters using density functional theory.

2. COMPUTATIONAL DETAILS

First-principle calculations have been performed using pseudopotential method, as implemented in the QUANTUM ESPRESSO/ PWSCF package [<http://www.pwscf.org>], within density functional theory (DFT) (Hohenberg and Kohn, 1964; Kohn and Sham, 1965). Our calculations are based on a plane-wave expansion method employing the local density approximation (LDA) for exchange and correlation term approximated by the Ceperley and Alder (1980) functional and parameterized by Vosko et al. (1980). During structure optimization, we have used a cubic super cell of edge size 24Å and periodic boundary conditions are imposed. The simulation cell size is taken to be large in order to avoid interaction of ions from the adjacent cells. The plane wave cut-off was set to be 210eV. In order to compare the results for various sizes, the Cadmium Telluride clusters are simulated with different number of Cadmium and Telluride paired atoms. We have employed conjugate gradient (CG) technique implemented for optimizing geometry. The valence electron configurations used for Cd, Zn and Te are $5s^24d^{10}$, $4s^23d^{10}$ and $5s^25p^4$ respectively. In all the structure optimizations, the force and energy convergence considered are 10^3 eV/Å and 10^4 eV respectively.

3. RESULTS AND DISCUSSION

A major feature of semiconductor nanocrystals is the quantum confinement effect, which leads to spatial enclosure of the electronic charge carriers within the nanocrystals. Because of this effect, the size and shape of these artificial atoms widely and precisely tune the energy of discrete electronic energy states and optical transitions. These particles also span the transition between small molecules and bulk crystals. In the size regime of the nanocrystals where the size approaches the exciton (i.e. electron hole pairs) Bohr radius, the bulk semiconductor band

structure with a continuum of energy states evolve into a set of discrete atomic-like energy states. Therefore, by simply changing the nanocrystal size, the optical properties of the material can be tuned (Swati, 2001). As the number of atoms in the particle increases, the discrete energies of the molecular orbitals merge toward a pseudo continuum of energy levels, converging to the solid state band-structure of the bulk material. The highest occupied molecular orbital minus the lowest unoccupied molecular orbital (HOMO-LUMO gap) energy increases with decreasing number of atoms in the cluster. This increasing energy difference as the size of the nanoparticle decreases is known as the quantum size effect. In this account, we discuss the structural and electronic properties of zinc doped and undoped cadmium telluride clusters, Cd_nTe_n ($n = 1-7$), and compare our calculations with other available similar results.

3.1. Structural Properties of Cadmium Telluride (Cd_nTe_n) and Cadmium Zinc Telluride ($Cd_{(n-m)}Zn_mTe_n$) Clusters

For the electronic structure calculations, we considered the binding energy, HOMO-LUMO energy gap and the second order energy difference explained below. The binding energy (BE) is the amount of energy released at its creation or the amount of energy we need to add to the system in order to break it up. So for, the cluster Cd_nTe_n , the binding energy per atom is calculated by using (Yonas and Hagos, 2014),

$$BE = \frac{n[E(Cd) + E(Te)] - E(Cd_nTe_n)}{2n} \quad (1)$$

Where, $E(Cd_nTe_n)$ is the lowest energy structure for Cd_nTe_n cluster, $E(Cd)$ and $E(Te)$ are the energies of the cadmium and telluride atoms respectively and n is the number of CdTe units.

This is used for hetrostructure, that is, made by two different atoms. For the Zn doped CdTe system, we use the following formula,

$$BE = \frac{(n-m)E(Cd) + nE(Te) + mE(Zn) - E(Cd_{(n-m)}Zn_mTe_n)}{2n} \quad (2)$$

where $E(Zn)$ is energy of zinc atom and $E(Cd_{(n-m)}Zn_mTe_n)$ is energy of $Cd_{(n-m)}Zn_mTe_n$ clusters for $n = 1 - 7$ and $m = 0 - 3$.

There is another way of identifying the stability of clusters in cluster physics, that is, the second-order energy difference. The second-order energy difference is a sensitive quantity that reflects

the relative stability of cluster and can be directly compared with the experimental relative abundance and it can be calculated using (Hagos and Anjali, 2007),

$$\Delta^2 E = E_{(n-1)} + E_{(n+1)} - 2E_{(n)} \quad (3)$$

where $E_{(n-1)}$, $E_{(n+1)}$ and E_n represent the total energy of the lowest energy structure $\text{Cd}_{(n-1)}\text{Te}_{(n-1)}$, $\text{Cd}_{(n+1)}\text{Te}_{(n+1)}$ and Cd_nTe_n clusters respectively.

The energy difference between the HOMO and LUMO reflects the ability for electrons to jump from occupied orbital to unoccupied orbital and represents the ability for the molecular orbital to participate in the chemical reactions to some extent. A larger HOMO-LUMO gap corresponds to a weaker chemical activity (Swati, 2001). This HOMO-LUMO gap energy is obtained by using equation (4):

$$E_g = (\text{HOMO} - \text{LUMO})_{(\text{gap})} = E_{(\text{LUMO})} - E_{(\text{HOMO})} \quad (4)$$

Optimized geometry structures for Cd_nTe_n for $n = 1-7$ clusters are shown in figure 1.

3.1.1. CdTe dimer

Cd-Te bond length of CdTe dimer is found to be 2.50\AA which is in good agreement with the results obtained from GGA-PBE calculation found by Bhattacharya and Anjali (2007) 2.57\AA and the binding energy calculated using equation (1) is 0.95eV . The HOMO-LUMO gap energy calculated using equation (4) is 0.27eV .

3.1.2. Cd₂Te₂ cluster

The lowest energy structure of this cluster attains a rhombus planar geometry. The Cd-Te bond length is found to be 2.69\AA and that of Cd-Cd is 2.73\AA . It favors ionic bonding due to the alternatively placed cadmium and telluride atoms in the cluster. Thus, the cluster has higher binding energy of 1.92eV per atom. This is due to the additional homonuclear Cd-Cd bonding. The HOMO-LUMO gap of this cluster is found to be 1.28eV . It has two isomers that are first local minima in a square structure and second local minima in a rhombic planar structure with energy difference of 0.54eV and 1.03eV respectively; normalized to lowest energy structure.

3.1.3. Cd₃Te₃ cluster

This cluster presents alternate cadmium and telluride atoms, with three telluride atoms edge-capping. The Cd atoms form an equilateral triangle of side 3.19\AA whereas the Cd-Te bond length is found to be 2.62\AA . The binding energy per atom of this cluster is calculated to be 2.31eV and

the HOMO-LUMO gap is 2.30eV. From the above discussion, Cd_3Te_3 cluster has a greater binding and HOMO-LUMO energy gap.

3.1.4. Cd_4Te_4

The lowest energy structure of this cluster is a three dimensional (rhombohedral) structure made of two rhombus structure (Cd_2Te_2), joined in a Cd, Te alternating fashion. The average Cd-Te bond length is calculated to be 2.80Å and this value is agreed with the bulk bond length 2.81Å (Bhattacharya and Anjali, 2007). The Cd-Te bond length increases as compared with that of the Cd_3Te_3 and this might be due to the increase in coordination number. The binding and HOMO-LUMO gap energy of this cluster are found to be 2.37eV and 2.01eV respectively.

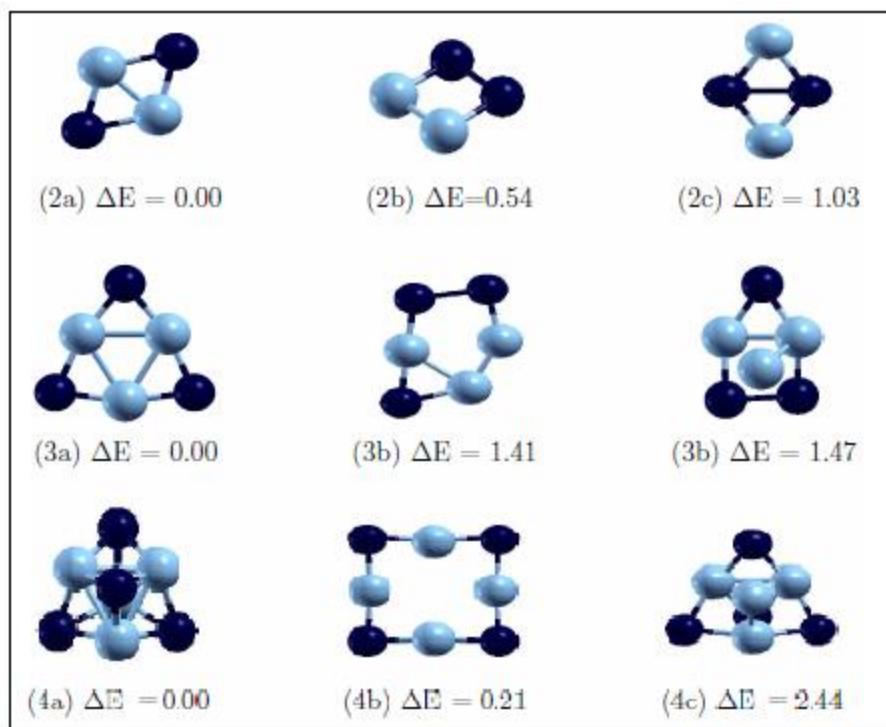


Figure 1. Optimized geometries for Cd_nTe_n clusters for $n = 1 - 4$. (a) denote the lowest energy structures, (b) denote the next lowest energy structure (first isomer) and in (c) are the second isomers. Numbers at the bottom of each cluster represent total energy difference, in eV, with respect to the lowest energy structure. (Dark color represents Te atom and the other is Cd atom).

From figure 1, we observe that, the isomers are found with the energy difference of 0.21eV and 2.44eV respectively with respect to the lowest energy configuration. The first isomeric structure is a square planar structure with Cd and Te atoms in an alternating arrangement, while the

second isomeric structure is found by capping Cd and Te on the triangular structure of the lowest energy structure of Cd_3Te_3 cluster as illustrated in figure 1.

3.1.5. Cd_5Te_5

The lowest energy structure is found from three rhombic and two triangular structures with an average CdTe bond length of 2.76Å. It is derived from Cd_4Te_4 cluster by adding CdTe dimer along the negative x-direction. The binding and the HOMO-LUMO energy gap of this cluster are calculated to be 2.44eV and 1.56eV respectively. As shown in figure 2, it has first and second lowest minimum energy structures with the energy difference of 1.18eV and 2.45eV respectively with respect to the lowest energy structure. The first lowest minimum energy structure is planar.

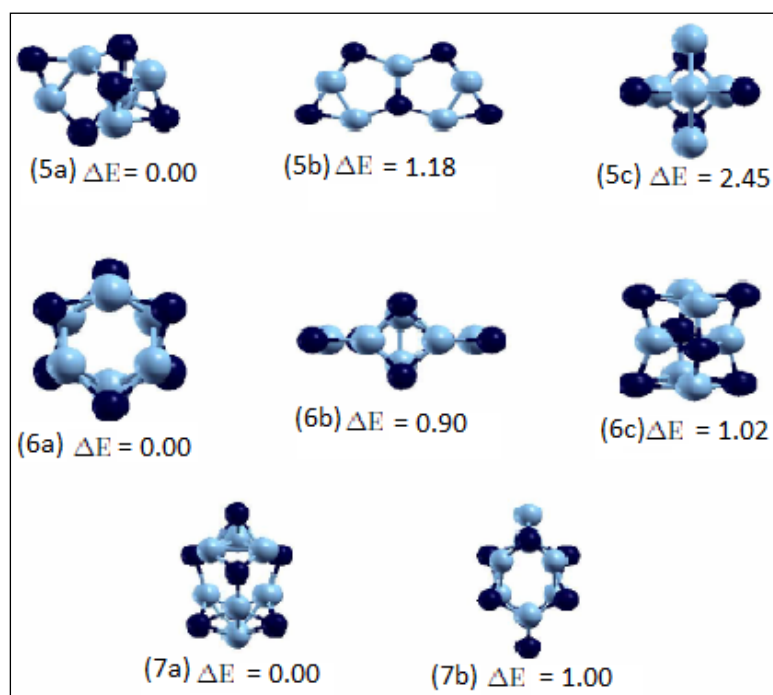


Figure 2. Optimized geometries for Cd_nTe_n clusters for $n = 5 - 7$. (a) denote the lowest energy structures, (b) denote the next lowest energy structure (first isomer) and in (c) are the second isomers. Numbers at the bottom of each cluster represent total energy difference, in eV, with respect to the lowest energy structure. (Dark color denote Te atom and the other is Cd).

3.1.6. Cd_6Te_6

The lowest energy structure is a hexagonal structure built from two parallel triangular structures joined together by six rhombus structures from a side. Its average Cd-Te bond length is found to

be 2.77\AA with the binding and HOMO-LUMO energy gap of 2.54eV and 1.86eV respectively. Its first and second lowest minimum energy structures are both three dimensional.

3.1.7. Cd_7Te_7 cluster

This structure is obtained by capping Cd on one of the surfaces of Cd_6Te_6 polyhedron as shown in figure 2 (7a), Te on the other surface. As a result, six Cd_2Te_2 and three Cd_3Te_3 structures are found in the lowest energy structure. The average Cd-Te distance is calculated to be 2.76\AA and the binding energy per atom of this cluster is found to be 2.55eV with the HOMO-LUMO gap of 1.96eV . We include one higher energy structure with an energy difference of 1.0eV .

As shown in figures 1 and 2, the lowest energy structures are all three dimensional (except for $n = 2$ and 3) which are made up of rhombic and triangular structures. Moreover, we observe that, Cd_4Te_4 and Cd_6Te_6 clusters are more symmetric and compact than the other clusters. From the lowest energy structure of Cd_nTe_n clusters discussed above and are shown in figures 1 and 2, we observe two basic building blocks in the construction of the structures, i.e. rhombic Cd_2Te_2 and triangular Cd_3Te_3 with Cd-Te bond alternative arrangement. As the cluster size increases from Cd_5Te_5 to Cd_7Te_7 , the number of triangular structure or Cd_3Te_3 clusters also increases. Therefore, the lowest-energy structure consisting of Cd_3Te_3 with CdTe alternative arrangement can be viewed as the embryo of zinc-blende structure of cadmium telluride crystal. Moreover, because of the intensive direction-properties of the CdTe covalent bond, there is no radical change in the structures for Cd_nTe_n clusters for $n = 6$ and 7 . This result agrees with the work of Jianguang (2009) except for Cd_4Te_4 and Cd_5Te_5 clusters in which they obtained planar structures as a lowest energy but in this study, the structure of these clusters are three dimensional as mentioned above. The difference might be the method they applied GGA-PBE. In general, the average Cd-Te bond length of the studied clusters is less than that of the bulk CdTe crystal, 2.81\AA . This might be due to the incomplete coordination in these clusters on account of very small number of atoms. The bond length of CdTe dimer is the smallest. The average Cd-Te bond length shrinks with increasing n in the planar structures, $n = 1 - 3$ and increases in going from planar to 3D structures.

3.2. Lowest Energy Structures of $(\text{Cd}_{(n-m)}\text{Zn}_m\text{Te}_n)$, for $n = 1 - 7$ and $m = 0 - 3$ clusters

Similar to the cadmium telluride bare clusters, we have performed energy optimization of cadmium zinc telluride clusters. The optimized structures of $(\text{Cd}_{(n-m)}\text{Zn}_m\text{Te}_n)$ clusters for $n = 1 -$

7 and $m=0 - 3$, with the condition that $n-m \geq m$ displayed in figure 3 are similar to the corresponding structures of bare Cd_nTe_n clusters, discussed in the previous section. But we have found different values of Zn-Te bond length after doping as compared with Cd-Te bond length in the bare Cd_nTe_n clusters.

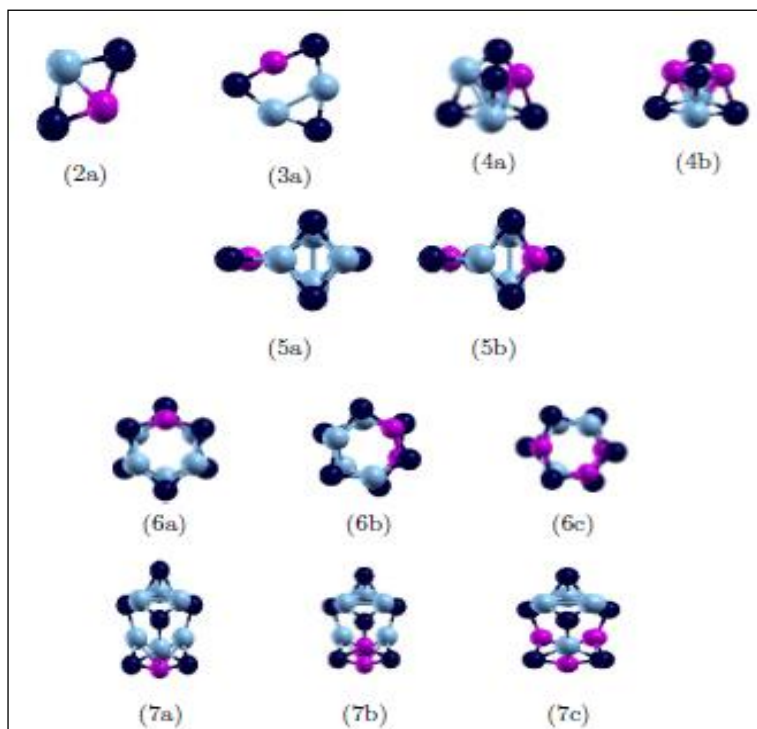


Figure 3. Optimized geometries of $(\text{Cd}_{(n-m)}\text{Zn}_m\text{Te}_n)$ for $n = 1-7$ and $m = 0-3$. (a) denotes optimized geometries of Monodoped ($m = 1$) (b) denotes the optimized geometries of Bi-doped ($m = 2$) and (c) denotes optimized geometries of tri-doped ($m = 3$). Numbers at the bottom indicate the cluster size (n). (Dark color represent Te, dark gray (online red) represents Zn, and gray is for Cd atom.).

In the optimized structures of bare and Zn doped Cd_nTe_n clusters, we have observed that, the Te atoms prefer to stay on the peripherals of the clusters while Cd atom prefer to go inside the cluster in relative sense. Comparing the preference of Cd and Zn atoms in $\text{Cd}_{(n-m)}\text{Zn}_m\text{Te}_n$ clusters, it is found that, Zn shows more tendency to go inside the clusters as compared with Cd atoms. This may be due to the difference in atomic radius and electronegativity of the atoms. The atomic radius of Cd, Zn and Te atoms are respectively, 1.71\AA , 1.53\AA and 1.42\AA and the electronegativity of Cd, Zn and Te atoms are 1.52eV, 1.59eV and 2.16eV (Miessler and Tarr, 2003). These results are analyzed by observing the structures formed and by comparing the bond

angles and bond length between the atoms. Thus, the angle at $\hat{Te} < \hat{Cd} < \hat{Zn}$ is due to the difference in lone pair electrons. This implies that, Zn atom moves inward more than Cd atom and Te atom moves outward compared with Cd and Te atoms.

3.3. Electronic Properties of Cadmium telluride and Cadmium zinc telluride Clusters

One of the main goals in cluster physics is to search for stable individual units that can serve as the elementary building blocks for electronic and optical nano devices. This stability can be verified in terms of energy such as binding energy, second order energy difference and HOMO-LUMO gap energy. In this section, we have discussed the average Cd-Te and Zn-Te bond lengths, binding energy(BE), the HOMO-LUMO(HL) gap, second order energy differences (SOED), density of states (DOS) and partial charge density of cadmium telluride and cadmium zinc telluride clusters.

Table 1. The average Cd-Te bond length (in Å) of Cd_nTe_n and $Cd_{n-m}Zn_mTe_n$ clusters, for $n = 1 - 7$ and $m = 0 - 3$.

| Size, (n) | L(m = 0) | L(m = 1) | L(m = 2) | L(m = 3) |
|-----------|----------|----------|----------|----------|
| 1 | 2.50 | | | |
| 2 | 2.69 | 2.70 | | |
| 3 | 2.62 | 2.62 | | |
| 4 | 2.80 | 2.80 | 2.80 | |
| 5 | 2.76 | 2.79 | 2.79 | |
| 6 | 2.77 | 2.77 | 2.78 | 2.77 |
| 7 | 2.76 | 3.77 | 3.77 | 2.77 |

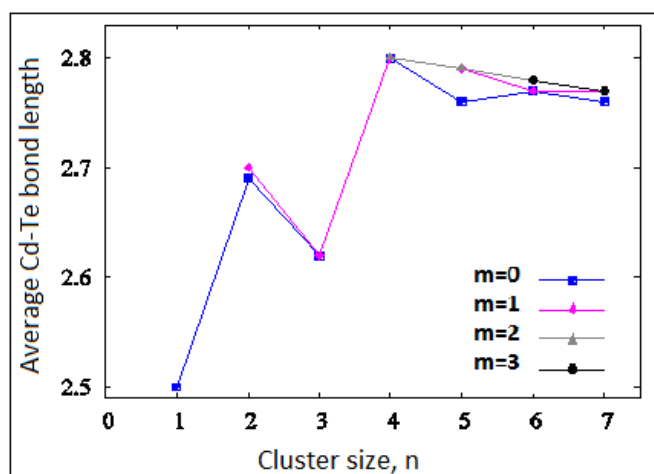


Figure 4. Graph of average Cd-Te bond length (in Å) of Cd_nTe_n and $Cd_{(n-m)}Zn_mTe_n$ clusters, versus cluster size, n clusters, for $n = 1 - 7$ and $m = 0 - 3$.

The variation of Cd-Te bond length in the Zn doped clusters as compared with the undoped Cd_nTe_n clusters is found to be insignificant except for $n = 5$ as shown in figure 4. However, it is found in this work that, the Zn-Te distance in the doped clusters is different from the Cd-Te bond length due to the reasons given above, that is, ionic radius and electronegativity of the atoms.

Figure 4 shows the average bond length of Cd-Te in doped and undoped Cd_nTe_n clusters. From this figure, the average bond length in bare CdTe oscillates with increasing cluster size. The Cd-Te bond length shows a dip at Cd_3Te_3 and Cd_2ZnTe_3 clusters. This might be due to the change in coordination number from two to three dimensional when compared with doped and undoped Cd_4Te_4 clusters. Thus, we can say that, these clusters might be stable clusters compared with the other clusters. The calculated values are shown in table 1. If the cluster size increases in a planar structure, then, its bond length decreases. Most of the time, these planar structures make ionic bonds which have shorter bond lengths due to their strong force of attraction rather than covalent bonds. Our calculation shows that CdTe and ZnTe are most ionic clusters.

The binding energy of Zn doped and undoped Cd_nTe_n clusters are calculated using equation (1) and equation (2) and are given in table 2. Our calculation shows that, the binding energy of Cd_nTe_n clusters increases with increasing cluster size and this may be due to the increase in coordination number. For the Zn doped clusters, the binding energy increases with increasing the level of dopant. This effect is as a consequence of the decrease of Zn-Te bond length (dimer 2.32Å) as compared with Cd-Te bond length (dimer 2.50Å), this means, zinc atom has smaller covalent radius than cadmium atom. Moreover, figure 5 shows that, the Zn doped Cd_nTe_n clusters binding energy curve is enhanced for $n = 7$ which can be considered as the most stable cluster. At Cd_nTe_n the binding energy of the Zn doped clusters is slightly greater than the corresponding undoped clusters and increases with increasing the number of doped atoms.

As was discussed before, one way of identifying the stability of the clusters is second-order energy difference. The second-order energy difference of monodoped and undoped clusters are calculated using equation (3) and the results are displayed in table 3 and figure. 6. As a result, doped and undoped Cd_3Te_3 and Cd_6Te_6 clusters show peak values as compared with their neighboring clusters. Hence, we can say that, these clusters are more stable than the other clusters.

Table 2. The binding energy per atom ,in eV, of Cd_nTe_n and $Cd_{(n-m)}Zn_mTe_n$ clusters as a function of cluster size n, for $n = 1 - 7$ and $m = 0 - 3$.

| Size, (n) | E(m = 0) | E(m = 1) | E(m = 2) | E(m = 3) |
|-----------|----------|----------|----------|----------|
| 1 | 0.95 | | | |
| 2 | 1.92 | 2.02 | | |
| 3 | 2.31 | 2.37 | | |
| 4 | 2.37 | 2.42 | 2.47 | |
| 5 | 2.44 | 2.48 | 2.52 | |
| 6 | 2.54 | 2.57 | 2.60 | 2.63 |
| 7 | 2.55 | 3.01 | 3.04 | 3.10 |

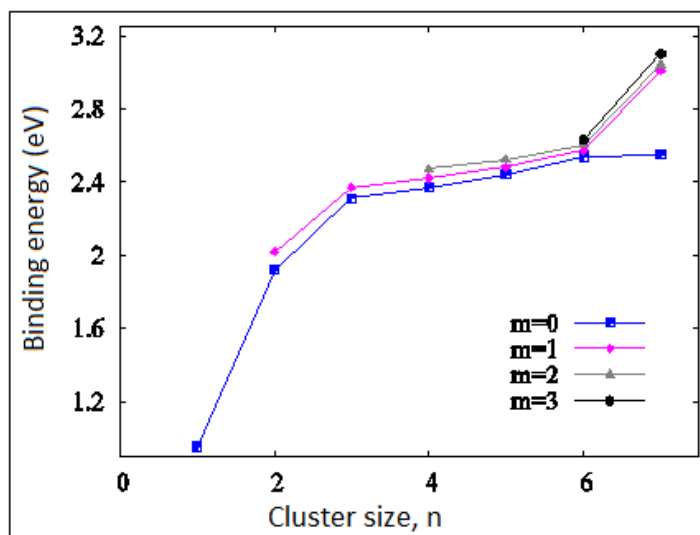


Figure 5. Graph of binding energy of Cd_nTe_n and $Cd_{(n-m)}Zn_mTe_n$ clusters verses cluster size, n clusters, for $n = 1 - 7$ and $m = 0 - 3$.

Table 3. The second-order energy difference $\Delta^2E(m = 0)$ for the undoped Cd_nTe_n cluster and the monodoped, $Cd_{(n-1)}ZnTe_n$ clusters, for $n = 1 - 7$.

| Size, (n) | $\Delta^2E(m = 0)$ | $\Delta^2E(m = 1)$ |
|-----------|--------------------|--------------------|
| 2 | -0.39 | |
| 3 | 1.01 | 0.97 |
| 4 | -0.21 | -0.25 |
| 5 | -0.72 | -0.64 |
| 6 | 0.96 | 0.77 |
| 7 | -0.74 | -0.60 |

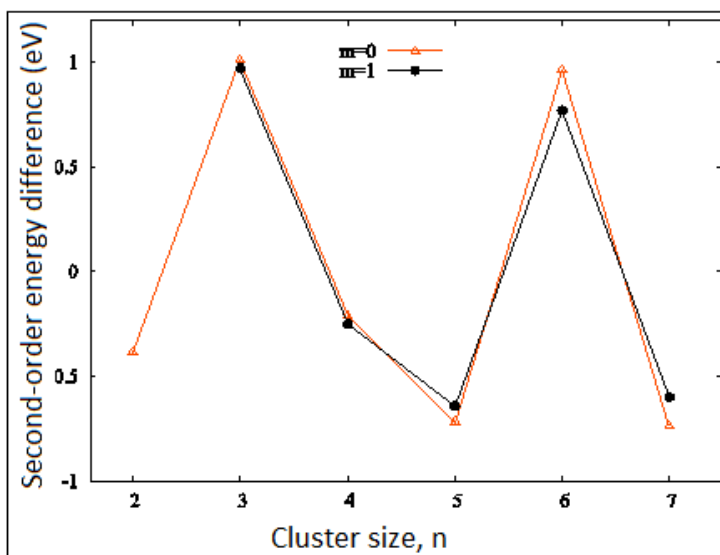
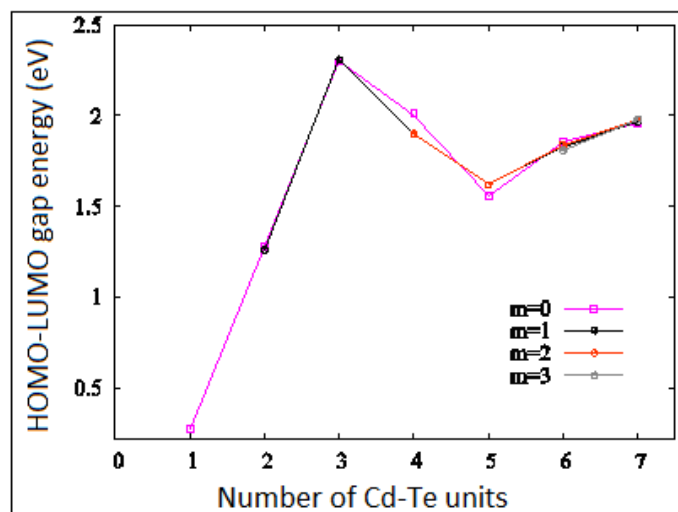


Figure 6. The second-order energy difference $m = 0$ for the undoped Cd_nTe_n clusters and the monodoped, $\text{Cd}_{(n-1)}\text{ZnTe}_n$ clusters, for $n = 1 - 7$.

For the optimized configurations of doped and undoped Cd_nTe_n clusters, the HOMO-LUMO energy gaps are computed and summarized in table 4. Clusters which have large HOMO-LUMO gap are more stable than those with lower values. The results shown in figure 7 are the HOMO-LUMO gaps of those optimized cadmium telluride Cd_nTe_n and cadmium zinc telluride clusters which do not show perfect odd/even oscillation. The HOMO-LUMO energy gap of bare Cd_nTe_n clusters is included for comparison. From this figure, we can conclude that, as the cluster size increases, there is a tendency of increasing HOMO-LUMO gap which results in a less chemical reactivity. It is worthy to point out that, the HOMO-LUMO gap is also considered as an important parameter to estimate the electronic stability of small clusters. The larger energy gap indicates more electronic stability and less reactivity and vice versa. Therefore, in figure 7 the highest peak of HOMO-LUMO gaps appear at the Cd_3Te_3 and Cd_2ZnTe_3 clusters with the values of 2.30eV and 2.31eV respectively, implying that, these clusters possess the highest electronic stability than the other clusters. HOMO-LUMO gap of the doped and undoped Cd_nTe_n , for $n > 2$ varies in the range of 1.26eV to 2.31eV which is in the range of the semiconductor band gap. The low HOMO-LUMO gaps appear at CdTe dimer.

Table 4. HUMO-LUMO energy gap, (in eV), of Cd_nTe_n and $Cd_{n-m}Zn_mTe_n$ clusters, for $n = 1 - 7$ and $m = 0 - 3$.

| Size, (n) | H(m = 0) | H(m = 1) | H(m = 2) | H(m = 3) |
|-----------|----------|----------|----------|----------|
| 1 | 0.27 | | | |
| 2 | 1.28 | 1.26 | | |
| 3 | 2.30 | 2.31 | | |
| 4 | 2.01 | 1.90 | 1.88 | |
| 5 | 1.56 | 1.62 | 1.62 | |
| 6 | 1.86 | 1.83 | 1.84 | 1.81 |
| 7 | 1.96 | 1.97 | 1.98 | 1.98 |

Figure 7. HOMO-LUMO energy gap (in eV) of Cd_nTe_n and $Cd_{(n-m)}Zn_mTe_n$ clusters, for $n = 1 - 7$ and $m = 0 - 3$, as a function of cluster size (n).

3.4. Partial Charge Density Analysis

To describe the nature of bonding, delocalization of charge and other related properties, we have plotted isosurfaces of partial charge density plots of some representative clusters to bring out the contribution of each molecular orbital (MO) to the total charge density. It can be used to discuss the nature of individual molecular orbital, type of hybridization, overlap of molecular orbitals and delocalization of charge in the cluster and total charge density plots to understand the overall nature of bonding in the cluster.

3.4.1. CdTe/ZnTe

The bond length of CdTe and ZnTe dimers are found to be 2.50\AA and 2.32\AA which are smaller compared with the bulk values, with the binding energies of 0.95eV and 1.06eV respectively.

The HOMO-LUMO gaps are calculated to be 0.27eV and 0.42eV respectively, where the Fermi levels are within the gap, slightly above the HOMO levels as shown in figure 8. These variations might be due to the properties of Cd and Zn atoms such as the ionic and covalent radii increase in going from Zn to Cd whereas electronegativity and ionization energies decrease. Since the radius of Cd is greater than that of Zn, then the bond length of Zn–Te is smaller than that of Cd–Te. Moreover, the binding energy and HOMO-LUMO energy gap of ZnTe is greater as compared with CdTe and this might be as a consequence of greater ionization energy and electronegativity of Zn atom. Partial charge density distributions of the HOMO and LUMO orbitals of the CdTe and ZnTe dimers are shown in figure 8.

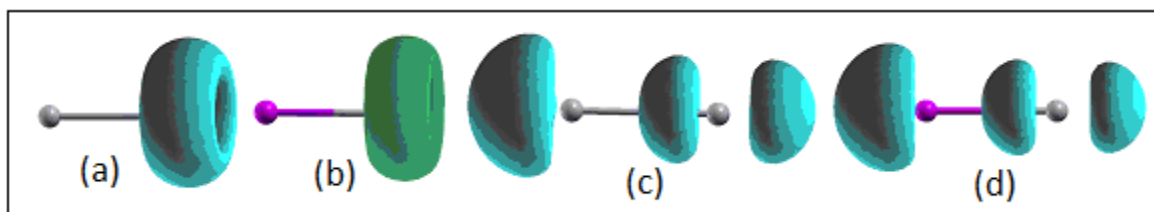


Figure 8. Partial charge density plots of the HOMO and LUMO orbitals of CdTe and ZnTe dimers. (a) and (b) are the HOMO of CdTe and ZnTe respectively and (c) and (d) show the LUMO of the two dimers respectively. Isosurfaces are plotted at $1/4^{\text{th}}$ of the maximum value.

Table 5. s, p and d partial charges with in Cd, Zn and Te spheres calculated for some occupied and unoccupied orbitals in CdTe, (left), and ZnTe, (right) dimers.

| Orbital | Atom | s | p | d | Orbital | Atom | s | p | d |
|---------|------|------|------|------|---------|------|------|------|------|
| HOMO | Cd | 0.00 | 0.02 | 0.01 | HOMO | Zn | 0.00 | 0.02 | 0.01 |
| | Te | 0.00 | 0.34 | 0.00 | | Te | 0.00 | 0.30 | 0.00 |
| LUMO | Cd | 0.08 | 0.10 | 0.01 | LUMO | Zn | 0.06 | 0.07 | 0.01 |
| | Te | 0.00 | 0.19 | 0.00 | | Te | 0.00 | 0.17 | 0.00 |

From figure 8, we observe that, the HOMO of CdTe and ZnTe dimers are localized on the Te atom while the LUMOs are distributed on both the Cd and Te atoms with more contribution from the Te atoms. The HOMO consists of Te *p* orbitals in both the dimers as shown in table 5. The LUMO of CdTe and ZnTe are found with the contribution of *s* and *p* orbitals of Cd and Te atoms to give *sp*-hybrid orbital which in turn forms a σ bond with the Te *p* orbital.

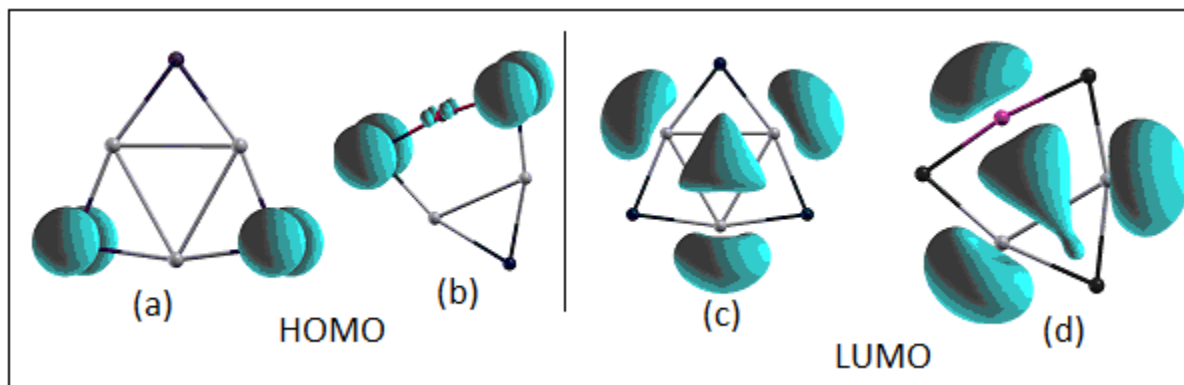


Figure 9. Partial charge density plots of orbitals around the Fermi level for Zn doped Cd_3Te_3 cluster and the bare Cd_3Te_3 for comparison. (a) and (c) are respectively HOMO and LUMO orbitals for Cd_3Te_3 and (b) and (d) are respectively LUMO orbitals for Cd_2ZnTe_3 clusters and Isosurfaces are plotted at $1/4^{\text{th}}$ of the maximum value. Cluster geometries are similar to figures 1(3a) bare and 3(3a) Zn doped.

Table 6. s, p and d partial charges within Cd, Zn and Te spheres calculated for some occupied and unoccupied orbitals in Cd_3Te_3 (a) and Cd_2ZnTe_3 (b).

| (a) | | | | | (b) | | | | |
|---------|------|------|------|------|---------|------|------|------|------|
| Orbital | Atom | s | p | d | Orbital | Atom | s | p | d |
| HOMO | Cd | 0.00 | 0.01 | 0.00 | HOMO | Cd | 0.00 | 0.01 | 0.00 |
| | Cd | 0.00 | 0.01 | 0.00 | | Cd | 0.00 | 0.01 | 0.00 |
| | Cd | 0.00 | 0.00 | 0.01 | | Zn | 0.00 | 0.00 | 0.02 |
| | Te | 0.00 | 0.18 | 0.00 | | Te | 0.00 | 0.00 | 0.00 |
| | Te | 0.00 | 0.18 | 0.00 | | Te | 0.00 | 0.16 | 0.00 |
| LUMO | Te | 0.00 | 0.00 | 0.00 | Te | 0.00 | 0.16 | 0.00 | |
| | Cd | 0.02 | 0.06 | 0.00 | LUMO | Cd | 0.02 | 0.08 | 0.00 |
| | Cd | 0.02 | 0.06 | 0.00 | | Cd | 0.02 | 0.08 | 0.00 |
| | Cd | 0.02 | 0.06 | 0.00 | | Zn | 0.01 | 0.06 | 0.00 |
| | Te | 0.00 | 0.00 | 0.00 | | Te | 0.01 | 0.00 | 0.00 |
| Te | 0.00 | 0.00 | 0.00 | Te | | 0.00 | 0.00 | 0.00 | |
| | Te | 0.00 | 0.00 | 0.00 | Te | 0.00 | 0.00 | 0.00 | |

3.4.2. $\text{Cd}_3\text{Te}_3/\text{Cd}_2\text{ZnTe}_3$

Figure 9 (a) and (b) show the HOMO of bare and Zn doped Cd_3Te_3 clusters respectively occupied at the two Te atoms, (c) and (d) show LUMO of bare and Zn doped Cd_3Te_3 clusters respectively occupied at the Cd atoms in the bare and Cd and Zn atoms in the doped cluster. It is found that, in these two clusters at the LUMO levels, charges are delocalized in the region between the atoms around the center. The detailed characteristics of partial charge distribution

for these orbitals is displayed in table 6 which shows the atomic contribution to some of the energy levels around the Fermi level.

In figure 9, the partial charge density plot of the LUMO and LUMO+1 orbitals of both clusters (bare and doped) show delocalization of charges at the center of the clusters indicating their semi-metallic nature. Due to same number of valence electrons in Cd and Zn atoms, there a similarity between the HOMO and LUMO orbital distributions in the bare and Zn doped clusters as clearly shown in figure 9 and table 6, which is also depicted in the dimers, figure 8 and table 5.

3.5. Density of States

The density of states of electrons in bands of different clusters yield the number of states in a certain energy range. Energy level diagrams of CdTe, ZnTe, Cd₃Te₃ and Cd₂ZnTe₃ clusters are displayed in figure10 where the Fermi level is found between the HOMO and LUMO levels, very near to the HOMO levels.

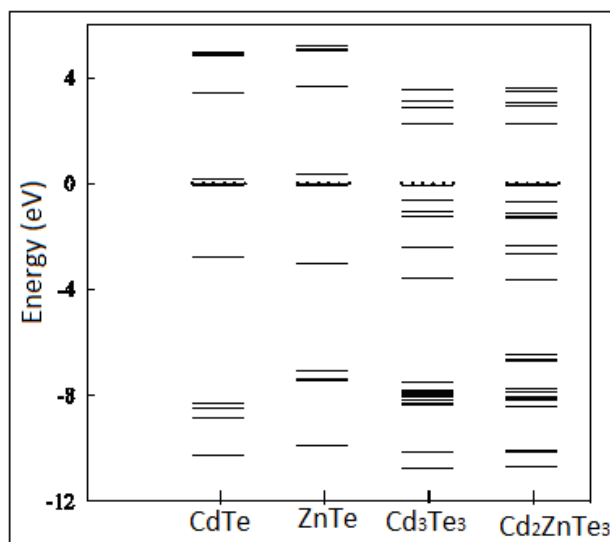


Figure 10. Energy levels of Cd₃Te₃ and Cd₂ZnTe₃ clusters. The discrete spectra are broadened by a Gaussian of width 0.01eV.

As is shown clearly in figure 10, the LUMO levels of the doped clusters are shifted up ward with respect to the position of LUMO of bare clusters due to the properties of Cd and Zn atoms explained above. The high density of energy levels around -8eV in Cd₆Te₆ cluster is observed to split into two groups with doping. As mention in Ali (2004) bond length and type of molecular orbitals are factors which affect the splitting of energy levels. The energy band gap of bulk CdTe

crystal has a calculated value of 1.49eV (Rusu, 2006). From the energy level plots of selected clusters, it can be concluded that, the energy level spectrum of small size clusters (CdTe and ZnTe) are more discrete than the large size clusters due to quantum confinement effect (Andrew and Shuming, 2010).

4. CONCLUSION

In this work structural and electronic properties of neutral and zinc doped cadmium telluride clusters are studied using QUANTUM ESPRESSO/ PWSCF package based on the principle of density functional theory (DFT), which in turn depends on pseudo-potential with a plane wave basis sets. The simulation of cadmium telluride and cadmium zinc telluride clusters is performed to study the size effect of the electronic and structural properties of the clusters. The lowest-energy structures of cadmium telluride clusters, Cd_nTe_n for $n = 1 - 7$ have been considered. Binding energy, bond length, band gap (HOMO-LUMO) gap energy, the LDOS for some of the clusters, partial charge density of the clusters are discussed. Upon geometry optimization, cadmium zinc telluride clusters get slightly inward and outward relaxations, with Cd and Zn atoms pulled in and Te atoms pushed out. From the results we found that, the lowest energy structure is planar for Cd_2Te_2 and Cd_3Te_3 clusters while the remaining are three dimensional. Telluride atoms prefer to be positioned on the peripheral sides of the cluster, while cadmium and zinc atoms favor to go inside a cluster. Our calculation shows that, the binding energy increases with increasing cluster size, the fact that constituent atoms in larger clusters have more neighbors resulting in strong interactions, i.e. the surface effect decreases with cluster size. In our simulation, doping of clusters is found to increase the binding energy for the same number of Te atoms in the cluster. In addition, the bond length also changes with cluster size. The bond length of Cd-Te dimer is greater than the bond length of Zn-Te dimer. Clusters of certain sizes often have special properties, i.e. higher stability or larger HOMO-LUMO gap when compared with other clusters, such as $Cd_{(3-m)}Zn_mTe_3$, for $m = 0, 1, 2$ clusters, according to the analysis of the binding energy, HOMO-LUMO gap and the second order energy difference. Thus, we can take it as a building block in the growth of the structures in our calculation. The partial charge density distribution of the HOMO and LUMO levels for Cd_nTe_n and $Cd_{(n-m)}Zn_mTe_n$ clusters show that the HOMO levels are predominantly localized on the Te atoms and the LUMO levels are

distributed on both Cd and Zn atoms. Moreover, the LUMO levels are delocalized at the center of the clusters due to the hybridization of molecular orbitals. The LDOS and energy level plots show discrete levels change in nearly continuous spectra with increasing cluster size. We recommend at this point in time that a further work be done for large cluster size to see better characteristics of the clusters for practical applications using experiment and a high computing facility.

5. ACKNOWLEDGEMENTS

The authors would like to thank the Department of Physics at the College of Natural and Computational Sciences, Mekelle University, Ethiopia, for providing computational facilities to conduct the research work. The first author wants to thank the Ministry of Education of the Democratic Republic of Ethiopia for the financial support.

6. REFERENCE

- Ali Omar, M. 2004. Elementary solid State Physics. Pearson Education, Inc., 176p.
- Andrew, M. S & Shuming, N. 2010. Semiconductor Nanocrystals: Structure, Properties and Band Gap Engineering. *Acc. Chem. Res.*, **43(2)**: 190–200.
- Bhattacharya, S.K & Anjali, K. 2007. Ab-initio Calculations of Structural and Electronic Properties of CdTe Clusters. *Phy. Rev.*, **B 75**: 035402.
- Ceperley, D.M & Alder, B. J. 1980. Ground State of the Electron Gas by a Stochastic Method. *Phys. Rev. Lett.*, **45**: 566.
- Douglas L. S., Martin, P., Doug, H. R., Ed Urgiles., Andrew, F. C., David, W. N., Kim M. J., Randy J. E., Calvin J. C & David S. G. 1997. CdTe Thin Films from Nanoparticle Precursors by Spray Deposition. *Chem. Mater.*, **9**: 889-900.
- Hagos, W & Anjali, K. 2007. How Cationic Gold Clusters respond to a single sulfur atom? *J. Chem. Physics*, **127(22)**: 224708.
- Hohenberg, P & Kohn, W. 1964. Inhomogeneous Electron Gas. *Phys. Rev.*, **136**: B864.
- <http://www.pwscf.org>, (PWSCF code in Quantum-Espresso).
- Jianguang, W. 2009. Structural growth behavior and polarizability of CdTe clusters. *Journal of Chemical Physics*, **130**: 214307.

- Kohn, W & Sham, L. 1965. Self-Consistent Equations Including Exchange and Correlation Effects. *Journal of Phys. Rev.*, **140**: A1133.
- Miessler, G.L & Tarr, D. A. 2003. Inorganic Chemistry. 3rd edition, Pearson Education, India 673p.
- Rusus, G.G. 2006. Structural, Electronic Transport and Optical Properties of Zn-Doped CdTe Thin Films. *Journal of Optoelectronics and Advanced Materials*, **8**: 931 - 935.
- Shreekanthan, K. N. 2006. Structural and Properties of Vacuum Deposited Cadmium Telluride Thin Films, *Indian Journal of Pure & Applied Physics*, **44**: 706-708.
- Swati, J. 2001. Photoluminescence Study of Cadmium Zinc Telluride. MSc Thesis, West Virginia University, Eberly College of Arts and Sciences (unpubl.).
- Vosko, S.H., Wilk, L & Nusair, M. C. 1980. Accurate spin-dependent electron liquid correlation energies for local spin density calculations: a critical analysis. *J. Phys.*, **58**:1200.
- Yonas, M & Hagos, W. 2014. Structural evolution and stabilities of (PbTe)_n(n=1-20) clusters. *Computational and Theoretical Chemistry*, **1039**: 40-49.